THE JOURNAL OF BIOLOGICAL CHEMISTRY VOL. 290, NO. 37, pp. 22771–22781, September 11, 2015

Acute and Temporal Expression of Tumor Necrosis Factor (TNF)-α-stimulated Gene 6 Product, TSG6, in Mesenchymal Stem Cells Creates Microenvironments Required for Their Successful Transplantation into Muscle Tissue*

Received for publication, December 4, 2014, and in revised form, July 13, 2015 Published, JBC Papers in Press, July 15, 2015, DOI 10.1074/jbc.M114.629774

Shigeko Torihashi[‡], Mioko Ho[§], Yuji Kawakubo[§], Kazumi Komatsu[§], Masataka Nagai[§], Yuri Hirayama[§], Yuka Kawabata[‡], Nana Takenaka-Ninagawa[‡¶], Orawan Wanachewin[‖], Lisheng Zhuo[‖], and Koji Kimata[‖1]**

From the [‡]Department of Rehabilitation Sciences, Nagoya University Graduate School of Medicine, Nagoya 461-9673, Japan, the [§]Department of Physical Therapy, Nagoya University School of Health Sciences, Nagoya 461-8673, Japan, the [‖]Advanced Medical Research Center and Multidisciplinary Pain Center, Aichi Medical University, 1-1 Yazakokarimata, Nagakute, Aichi 480-1195, Japan, the [¶]Department of Clinical Application, Center for iPS Cell Research and Application, Kyoto University, Kyoto 606-8507, Japan, and the **Department of Biochemistry, Faculty of Medicine, Chiang Mai University, Chiang Mai 50200, Thailand

Background: Transplanted MSCs cannot settle in intact muscles.
Results: When MSCs release TSG6 in the intact muscle, they can settle after transplantation. TSG6 forms the SHAP-hyaluronan complex with hyaluronan and IαI.
Conclusion: TSG6, hyaluronan, and IαI are crucial factors forming footholds for the settlement and differentiation of MSCs.
Significance: TSG6, hyaluronan, and IαI serve for improvement of regenerative medicine.

Previously, we demonstrated that when mesenchymal stem cells (MSCs) from mouse ES cells were transplanted into skeletal muscle, more than 60% of them differentiated into muscles in the crush-injured tibialis anterior muscle *in vivo*, although MSCs neither differentiated nor settled in the intact muscle. Microenvironments, including the extracellular matrix between the injured and intact muscle, were quite different. In the injured muscle, hyaluronan (HA), heavy chains of inter-α-inhibitor (IαI), CD44, and TNF-α-stimulated gene 6 product (TSG-6) increased 24–48 h after injury, although basement membrane components of differentiated muscle such as perlecan, laminin, and type IV collagen increased gradually 4 days after the crush. We then investigated the microenvironments crucial for cell transplantation, using the lysate of C2C12 myotubules for mimicking injured circumstances *in vivo*. MSCs settled in the intact muscle when they were transplanted together with the C2C12 lysate or TSG6. MSCs produced and released TSG6 when they were cultured with C2C12 lysates *in vitro*. MSCs pretreated with the lysate also settled in the intact muscle. Furthermore, MSCs whose TSG6 was knocked down by shRNA, even if transplanted or pretreated with the lysate, could not settle in the muscle. Immunofluorescent staining showed that HA and IαI always co-localized or were distributed closely, suggesting formation of covalent complexes, *i.e.* the SHAP-HA complex in the presence of TSG6. Thus, TSG6, HA, and IαI were crucial factors for the settlement and probably the subsequent differentiation of MSCs.

Muscle injuries and fibrosis associated with movement impairment and pain are generally recognized as sequels that suffered from muscle detrition caused by accidents and unavoidable muscle damage during surgery of skeletal systems. Many reports in recent years have described that not only regeneration of impaired tissue but also reconstruction of lost tissues or organs could be performed by using mesenchymal stem cells (MSCs)[2] derived from one's own bone marrow, adipose tissues, ES cells, or iPS cells (1–5). Our previous report demonstrated that more than 60% of MSCs obtained from mouse ES cells had the potential to differentiate into skeletal muscles *in vivo* and revealed that the regeneration and functional recovery of injured muscle was possible by transplantation of MSCs (6, 7). However, MSCs neither differentiated nor settled in the muscle tissue when they were transplanted into intact muscles, as reported previously (7, 8). The observations suggested that microenvironments, including the extracellular matrix (ECM), are crucial for cell transplantation (9). If one is able to prove that ECM is required for MSC transplantation into intact tissue as a foothold, it should serve for efficient transplantation technology by reducing the loss of transplanted MSCs and preserve the precious cell population. Furthermore, if MSCs transplanted into the intact tissue are able to differentiate into muscle cells, muscle atrophy caused by immovability or disease may be remedied. The ECM required for the settlement of transplanted cells into the muscle tissue, however, has not been clearly demonstrated.

ECMs preferable for the differentiation and organogenesis of skeletal muscle tissues have been reported. Heparan sulfate and

* This work was supported in part by Japanese Government Grants-in-aid for Scientific Research (B) 22300185, Challenging Exploratory Research Grant 24650313 (to S. T.), and Scientific Research (C) Grant 23570148 (to K. K.). The authors declare that they have no conflicts of interest with the contents of this article.
[1] To whom correspondence should be addressed. Tel./Fax: 81-561-61-1898; E-mail: kimata@aichi-med-u.ac.jp.

[2] The abbreviations used are: MSC, mesenchymal stem cells; HA, hyaluronan; IαI, inter-α-trypsin inhibitor; SHAP, serum-derived hyaluronan-associated protein; TA muscle, tibialis anterior muscle; EGFP, enhanced GFP; DAMP, damage-associated molecular pattern.

chondroitin sulfate proteoglycan, hyaluronan (HA), tenascin-C, fibronectin, laminin, and other ECMs play crucial roles for skeletal muscle regeneration (9–17). In particular, TNF-α-stimulated gene 6 product (TSG6) with multiple functions is a key substance (16, 17). TSG6 was originally discovered in TNF-treated human fibroblasts and is expressed in a variety of cell types in response to inflammatory mediators. Protein TSG6 is not constitutively expressed in normal adult tissue but rather in inflammatory or inflammatory-like circumstances such as ovulation (18–20). By its link module, TSG6 can bind many substances such as glycosaminoglycan, including HA, to modulate the tissue microenvironment (21, 22). Heavy chains of inter-α-inhibitor (IαI) and HA were shown to form covalent complexes in the knee joint with rheumatoid arthritis (23). Formation reaction of the complex has recently been demonstrated to be mediated by the catalytic action of TSG6 (24, 25).

Successful transplantation is composed of two steps, *i.e.* cell settlement and their growth and differentiation. These steps proceed continuously but involve different mechanisms and factors. In this study, to clarify the environment required for foothold formation of MSCs in muscle tissues, we focused on the first step of transplantation. MSCs attach and adhere to muscle tissues that might be quite different between intact and injured muscle tissues. We then used the lysate of C2C12 myotubules for creating injured circumstances *in vivo* and *in vitro*, and we found that TSG6, HA, and IαI were crucial factors for the settlement of MSCs by creating the footholds of MSCs through TSG6-mediated formation of covalent complex between heavy chains of IαI and HA.

Experimental Procedures

Cells and Animals—G4-2 mouse ES cells, carrying the enhanced green fluorescent protein (EGFP) gene under the control of a cytomegalovirus/chicken β-actin promoter, was kindly gifted by Dr. H. Niwa, Riken Kobe, Japan. C2C12 mouse myoblasts were purchased from DS Pharma Biomedical (Osaka, Japan). Eight-week-old immunodeficient mice (SCID) were purchased from Japan Charles River (Yokohama, Japan) and used for the transplantation of MSCs, following the guidelines for the Animal Care and Use of the Nagoya University Graduate School of Medicine.

Culture and Sorting of Cells—ES cells were expanded in a culture medium termed ES-DMEM. The medium was composed of Dulbecco's modified Eagle's medium (Sigma) with 0.1 mM nonessential amino acids (Gibco), 1 mM sodium pyruvate (Gibco), 1 mM 2-mercaptoethanol (Sigma), and 0.5% of an antibiotic/antimycotic (Gibco) containing 10% fetal bovine serum (FBS; Biological Industries, Kibbuiz, Israel). For the expansion of cells, 1000 units/ml leukemia inhibitory factor (Chemicon, Temecula, CA) was added in ES-DMEM.

Generation of MSCs and their sorting were performed following our previously described protocol (6, 7). Briefly, ES cells were incubated for 2 days without leukemia inhibitory factor and compacted to form embryoid bodies in hanging drops. On the following 2 days, they were exposed to 10^{-7} M all-*trans*-retinoic acid (Sigma) in ES-DMEM, followed by washing for 2 days without all-*trans*-retinoic acid. After day 6, embryoid bodies were plated onto gelatin-coated dishes and then incubated with 1.7 μM insulin (Sigma) and 0.3 μM 3,3,5-triiodo-L-thyronine (Sigma) in ES-DMEM. Eight to 9 days after, embryoid bodies were detached from the dishes, dispersed using EDTA, and then sorted by a Magnetic Cell Separation System (Miltenyi Biotec, Auburn, CA) using both anti-CD105 antibody (R&D Systems, Minneapolis, MN) and anti-rat antibody conjugated with magnetic beads (Miltenyi Biotec). The process was conducted according to the manufacturer's instructions. $CD105^+$ cells thus obtained were transferred for culture to coating dishes as MSCs.

C2C12 murine myoblasts expanded their population in ES-DMEM containing 15% FBS followed by differentiation in low glucose-DMEM (Sigma D-6046) with 5% horse serum. After 7 days of differentiation, myoblasts differentiated into myotubes and were then collected into ES-DMEM without FBS. They were lysed by a sonicator Handy Sonic UR-20P (TOMY SEIKO, Tokyo, Japan) for 2.5 min at 4 °C. After that, the cell solution was incubated for 24 h at 37 °C under 5% CO_2. Then the solution was sterilized by filtration, and its protein concentration was measured. The solution was termed lysate of C2C12 and was added in the culture medium of MSCs at the protein concentration of 0.5 mg/ml.

Transplantation—Mice ($n = 40$) were anesthetized for surgery with subcutaneous injections of sodium pentobarbital (80 mg/kg). Skin on the tibialis anterior (TA) muscle was sterilized with 70% ethanol and then 0.5% benzalkonium chloride (Nihon-pharm. Co. Japan, Tokyo, Japan) and cut with a surgical blade. TA was exposed, and MSCs (1×10^5 cells in 20 μl of PBS) were injected into the mid-portions of the TA, and then the skin was sutured. In the case of injured muscle formation, TA muscles were crushed by direct clamping with a forceps for 1 min under the same and constant pressure. 24 h after the crush, MSCs were injected into the mid-portion of the injured area in TA. Mice receiving neither crushed nor injected treatment were processed as a control.

To examine conditions of the efficient cell transplantation, MSCs and/or 1 μg of recombinant mouse TSG6 (R&D Systems, 2326-TS-050), 10 μg of hyaluronan (HA; Altz Seikagaku Co., Tokyo, Japan), inter-α-inhibitor (IαI; 1.35 μg, purified from mouse serum), and lysate of C2C12 (5 μg as protein) in 10 μl of buffer solution were injected into the mid-portion of the TA muscle. Various combinations of cells and materials that were injected for the transplantation and the results of success (+) or failure (−) in the settlement of the injected cells were shown in Table 1.

Fluorescent Immunostaining and Image Acquisition—After 48 h of cell transplantation, mice were sacrificed and perfused with 10 ml of phosphate-buffered saline and then 4% paraformaldehyde, and fixed muscles were collected and immersed in 10–30% gradient sucrose phosphate-buffered saline overnight. The tissues were embedded in OCT compound (Tissue-Tec, Miami, FL) and frozen by immersing isopentane (Sigma) on liquid nitrogen. Muscle cryosections (10 μm thick) were cross-cut from the mid-portion of TA muscles (cell transplantation region) using a cryostat. Some sections were stained with hematoxylin and eosin (H&E), and others were processed for fluorescent immunostaining. Samples were incubated with the first antibodies followed by Alexa-labeled secondary antibodies as

TABLE 1

Transplantation of cells and materials

For mesenchymal stem cells, 1×10^5 cells were suspended in 20 μl of phosphate-buffered saline (PBS), pH 7.4, and injected for transplantation. For IαI, the preparation purified from mouse serum, 1.35 μg was dissolved in 10 μl of 50 mM Tris-HCl, pH 7.5, containing 0.15 M NaCl and injected. For HA, Altz (Seikagaku Corp.) (1 mg/ml PBS, pH 7.4), 10 μl was injected. For TSG6, recombinant mouse TSG-6 (R&D Systems, 2326 TS 050), 1 μg was dissolved in 10 μl of PBS, pH 7.4, and injected. For lysates, 5 μg of proteins of the C2C12 cell lysate in 10 μl of PBS, pH 7.4, was injected.

Conditions	Abbreviation	Pre-injection 6 h before cell transplantation	Transplantation condition of MSCs	Remaining MSCs
1	Control (MSCs)		MSCs only	−
2	MSCs + lysate		MSCs with lysate	+
3	Pre-lysate + MSCs	Lysate	MSCs	+
4	Treated MSCs		MSCs pre-treated with lysate for 6 hours	+
5	MSCs + TSG6		MSCs with TSG6	+
6	Pre-TSG6 + MSCs	TSG6	MACs	+
7	MSCs + IαI + HA		MSCs with IαI, HA	−
8	Pre-IαI, HA + MSCs	IαI and HA	MACs	−

TABLE 2

Antibodies for immunofluorescent staining

Primary antibody	Secondary antibody 1:400
Anti-human TSG6 antibody (N-20;sc21828)1:100 Santa Cruz Biotechnology	Alexa 594 donkey anti-goat IgG antibody Molecular Probes A11058
Anti-mouse ITI-H2 antibody (K-17; sc21978)1:100 Santa Cruz Biotechnology	Alexa 594 or Alexa 488 donkey anti-goat IgG antibody Molecular Probes A11058 or A11055
Biotinylated anti-HABP antibody 1:200 Seikagaku Biobusiness Corp.	Alexa 594 streptavidin Molecular Probes S11227
Anti-mouseCD44 antibody (CL8944AP) 1:50 Cedarlane	Alexa 594 goat anti-rat IgG antibody Molecular Probes A11007
Anti-EGFP/GFP antibody (OSE00003G)1:100 Osenses	Alexa 488 goat anti-rabbit IgG Molecular Probes A11008
Anti-GFP antibody (GTX26673)1:100 GeneTex	Alexa 488 donkey anti-goat IgG antibody Molecular Probes A11055
Anti-heparan sulfate 10E4 1:100 Sekagaku Biobusiness Corp., A80120	Alexa 594 goat anti-mouse IgM antibody Molecular Probes A21044
Anti-mouse perlecan HK102 1:50 Sekagaku Biobusiness Corp., AY0116	Alexa 594 goat anti-rat IgG antibody Molecular Probes A11007
Anti-Pax7 antibody (NBP1-52374) 1:100 Novus Biologicals	Alexa 594 donkey anti-goat IgG antibody Molecular Probes A11058
Anti-fetal actin (Ac20.4.2) 1:10 Progen	Alexa 488 donkey anti-mouse IgG antibody Molecular Probes A21202 or Alexa 488 goat anti-mouse IgG antibody Molecular Probes A11029
Anti-skeletal actin (E3884) 1:200 Spring Bioscience	Alexa 488 donkey anti-rabbit IgG antibody Molecular Probes A21206

shown in Table 2. When mouse IgG was used as a primary antibody, samples were treated with Vector M.O.M. immunodetection kit (Vector Laboratories, Burlingame, CA) according to the manufacturer's instructions. Some samples were counterstained with DAPI (1:1000; KPL, Gaithersburg, MD) just before mounting with Fluoromount^{TM} (DBS, Pleasanton, CA). Each time, the immunostaining was carried out under constant conditions. Sections were imaged using a microscope BZ-9000 (Keyence, Osaka, Japan) and were recorded and analyzed with a BZ-II analysis application (Keyence). For the measurement of the MSC area settled in the muscle, five cryosections widely stained with EGFP in each TA muscle were chosen, and EGFP-positive areas (35–255 pixels) were detected by dynamic cell count software in BZ-II analysis application. More than three animals were used for each condition (mean ± S.D.).

Western Blotting—As described above, MSCs ($CD105^+$ cells) were cultured on coating dishes. When the culture almost got confluent, C2C12 lysates were added to the medium to contain 0.5 mg/ml of the protein concentration, and the medium was collected after 12, 24, and 48 h of culturing, and control culture medium was also collected from MSCs continuously cultured in the normal medium for 48 h. The collected medium samples were concentrated by ethanol precipitation (23) and processed for Western blotting. The corresponding control culture media without lysate, and lysate of C2C12 itself, were also processed for Western blotting as described previously (23). Samples containing equal amounts of protein (20 μg) were mixed with the loading buffer (1% SDS, 50 mM Tris-HCl, pH 6.8, 4% 2-mercaptoethanol, and 20% glycerol), followed by boiling for 5 min. After electrophoresis, the proteins on the gel were electrotransblotted to a PVDF membrane (AE6667 ATTO, Tokyo, Japan). The membrane was treated with PBS-T containing 10% skim milk at 37 °C for 2 h to protect from nonspecific staining. For TSG6 immunostaining, the membrane was incubated with goat anti-human TSG6 antibody (1:1000 in PBS-T, see Table 2) and HRP-conjugated anti-goat immunoglobulin antibody (Nr.P 0160 Dako Japan, Tokyo, Japan; 1:2000 in PBS-T). For IαI immunostaining, the membrane was incubated with goat anti-mouse IαI antibody ITI-H2 (1:500 in PBS-T, see Table 2) and HRP-conjugated anti-goat immunoglobulin antibody (1:2000 in PBS-T). Finally, the immune complexes were visualized using enhanced chemiluminescence reagent Western

TABLE 3
Primers for real time PCR

Gene	Forward	Reverse	Product length
GAPDH	ATGTGTCCGTCGTGGATCTGA	TGCCTGCTTCACCACCTTCT	80
TSG6	GAGTCGGATACCCCATTGTGA	GAGCCGGATTCCATAATCGA	80

Lightning® Plus-ECL (NEL105001EA, PerkinElmer Life Sciences) and detected by a CCD camera system Ez-Capture ST (AE-9160PH, ATTO). Western blot probed densities were analyzed using ImagePro software. Integrated densities were normalized to the mock-treated serum signal at each time point (mean ± S.D.).

Real Time PCR—MSCs were first cultured in the normal medium, and after nearly reaching confluence, lysates of C2C12 were added as described above and further cultured for 3, 6, 9, 12, 24, and 48 h. As controls, MSCs continued being cultured in the normal medium for the corresponding time points. These cells were processed for real time PCR. Messenger RNAs were extracted by RNeasy kits (Qiagen, GmbH Germany) according to the manufacturer's instructions. After reverse transcription, the obtained cDNA was processed for real time PCR. The primers used were listed in Table 3. A mixture of SYBR Green (Thunderbird™ SYBR quantitative PCR mix; Toyobo, Osaka, Japan) was used with forward and reverse primers and a cDNA template. The comparative quantification was analyzed by a real time PCR system (StepOne Plus™, Applied Biosystems, Foster City, CA). Data normalization was accomplished using the GAPDH expression. Three independent experiments were performed. The purity of each PCR product was checked by analyzing the amplification plot and dissociation curves. Relative mRNA quantitation was calculated using the comparative C_T ($\Delta\Delta C_T$) method.

Knockdown of TSG6 by Short Hairpin (sh) RNA—A specifically designed shRNA vector was used to knock down mouse TSG6 expression in MSCs. Mouse unique 29-mer shRNA constructs in U6 plasmid vector pRFP-C-RS (TF517014C) and noneffective scrambled pRFP-C-RS vector were purchased from OriGene Technologies, Inc. (OriGene, Rockville, MD). The unique 29-mer nucleotide sequence was GATACTGTGGTGATGAACTTCCAGAAGAC. Knockdown by TSG6-specific shRNA into MSCs via transfection was performed according to the manufacturer's protocol. When MSCs grew and reached 70% confluence, plasmid DNA was added to the culture medium with TerboFection reagent (R0531 Thermo Scientific, Waltham, MA). 4 μg of plasmid DNA and 9 μl of TerboFection reagent were mixed into 4 ml of ES-DMEM in a 35-mm dish (BD Falcon) where the MSCs were plated. After 48 h of incubation, transfection was confirmed by red fluorescence, and then MSCs were used for experiments. The effect of knockdown by shRNA was confirmed by the measurement of TSG6-mRNA in MSCs.

Statistical Analysis—All experimental values were presented as means ± S.D. Statistical analysis was performed in all experiments by Excel and SPSS16.0 (SPSS Inc., Chicago, IL) software. Comparisons between groups were assessed by Student's *t* test. Adjustment for multiple comparisons was performed. Values of $p < 0.05$ were considered to be statistically significant.

Results

ECM in the Damaged TA as Microenvironments Specific to Skeletal Muscle Tissue Regeneration—Immunofluorescent staining of HA, IαI, and hyaluronan receptor CD44 indicated that their expressions were very low in control (intact) TA muscles (Fig. 1, *A* and *B*). Their increased expression was observed in the damaged TA muscle 24–48 h after the crush injury (Fig. 1, *C–H*). Some $CD44^+$ cells looked small and had nuclei at the center, similar to lymphocytes (26), and also expressed TSG6 (Fig. 1*D*, see details in the *inset*). The immunofluorescent staining showed that HA and IαI were distributed closely and often co-localized, suggesting that HA and the heavy chains of IαI formed a covalent complex, *i.e.* the SHAP-HA complex (Fig. 1*F*). The expression of HA and IαI, however, decreased afterward and reached nearly the control level 1 week later (Fig. 1*I*). In contrast, expressions of perlecan, laminin, and type IV collagen, which are typical basement membrane components and produced by differentiating skeletal muscle cells, were observed to increase gradually from 4 days after the crush, and reached maximum 1 or 2 weeks later (see example of heparan sulfate 10E4 and perlecan expression in Fig. 1, *J* and *K*). One week after the crush, Pax7 immunopositive nuclei indicating muscle stem and/or progenitor cells increased (Fig. 1, *L* and *M*). Considering those results together with other reports on changes in ECM during tissue degeneration and regeneration (9–18), we speculated that HA-rich matrices consisting of HA, the heavy chains of IαI, CD44, HA-binding chondroitin sulfate proteoglycans, heparan sulfate proteoglycans, as well as TSG-6 that appeared soon after injury may be a key environment that is temporally and specifically expressed in the damaged TA muscle.

Lysate of C2C12 Induces Settlement of MSCs Transplanted into Noninjured Muscle—We have shown before that the transplanted MSCs settled in the crushed TA muscles (7). However, MSCs did not settle when they were transplanted into noninjured TA muscle (Fig. 2*A, Con. 1*; Table 1). We assumed that some factors derived from injured muscle had induced the settlement of MSCs. It is well known that C2C12 is a myoblast cell line and can be easily differentiated into myotubules whose lysate was sometimes used as the microenvironment of injured muscles (8, 27) and could be prepared more easily and efficiently than from the injured muscles. We therefore examined whether the lysate of C2C12 showed such an activity. When the intact TA muscles received lysate of C2C12 (5 μg as protein in 10 μl of buffer solution) with MSCs, transplanted MSCs were able to settle at the injection areas (Fig. 2*A, Con. 2*; Table 1), supporting the above speculation. Injection of C2C12 lysate 6 h before MSC transplantation gave a significantly higher settlement efficiency than that of the simultaneous injection with MSC transplantation (Fig. 2, *A, Con. 3,* and *B*), which suggested

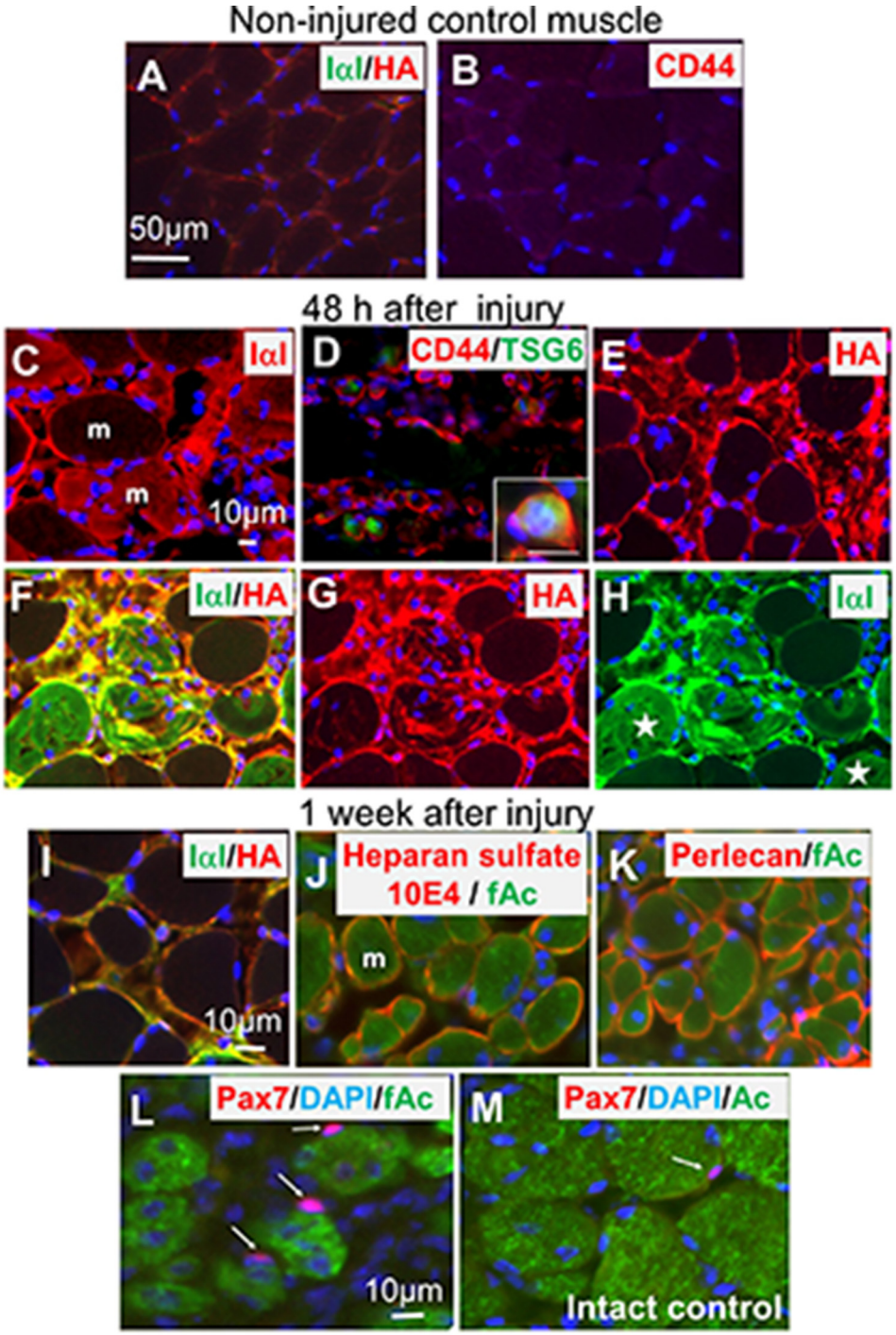

FIGURE 1. **ECM expression before and after injury of skeletal muscle tissue and Pax7 distribution.** In the control noninjured TA muscle Iαl in *green* and HA in *red* were not prominent (*A*). CD44 was also scarcely observed (*B*). Iαl (*C*), CD44 (*D*), and HA (*E*) in *red* increased soon after injury and peaked 24–48 h later. Some Iαl penetrated damaged muscle fibers shown in *red* (*C*). CD44 were expressed in the small cells. Some $CD44^+$ cells (*red*) also express TSG6 (*green*) (*D*). Details of the co-expression are shown in the *inset* of *D*. HA is expressed mainly in muscle matrix of the damaged area (*E*). Frequent co-localization (*F*) of Iαl (*green*) and HA (*red*) indicates the SHAP-HA complex formation was demonstrated. In individual images of Iαl (*G*) and HA (*H*) in *F*, some Iαl penetrated into the damaged muscle fibers (*stars*) and did not co-localize to HA that mainly located in the areas surrounding the muscle fibers. At the late stage of injury (1–2 weeks after injury), the SHAP-HA network decreased (*I*). However, heparan sulfate such as 10E4 (*J*) and perlecan (*K*) increased, and they surrounded the regenerating skeletal muscles expressing fetal actin (*green*). Pax7 immunopositive cells (*arrows*) increased and were closely located at the regenerating muscle fibers expressing fetal actin (*green*) (*L*). The population of $Pax7^+$ cells was higher than that of the intact control muscle expressing actin (*M*). *Scale bar* in *A* corresponds to *A* and *B*. *Scale bar* in *C* corresponds to *C–H*. *Scale bar* in insertion *D* is 10 μm. *Scale bar* in *I* corresponds to *I–K*. *Scale bar* in *L* corresponds to *L* and *M*. Counter-staining in *blue* by DAPI indicates nuclei. The mark *m* in *C* and *J* is muscle fiber, which was stained with fetal actin antibody as shown in *J* and *K*.

that the C2C12 lysate had the capacity to create the microenvironment formed in the injured muscle tissues as described above, which contained the HA-rich matrices (Fig. 2, *C* and *D*).

We next examined the effects of C2C12 lysate on MSCs. They were cultured in a medium containing the lysate of C2C12 for 6 h before transplantation and were able to settle in the

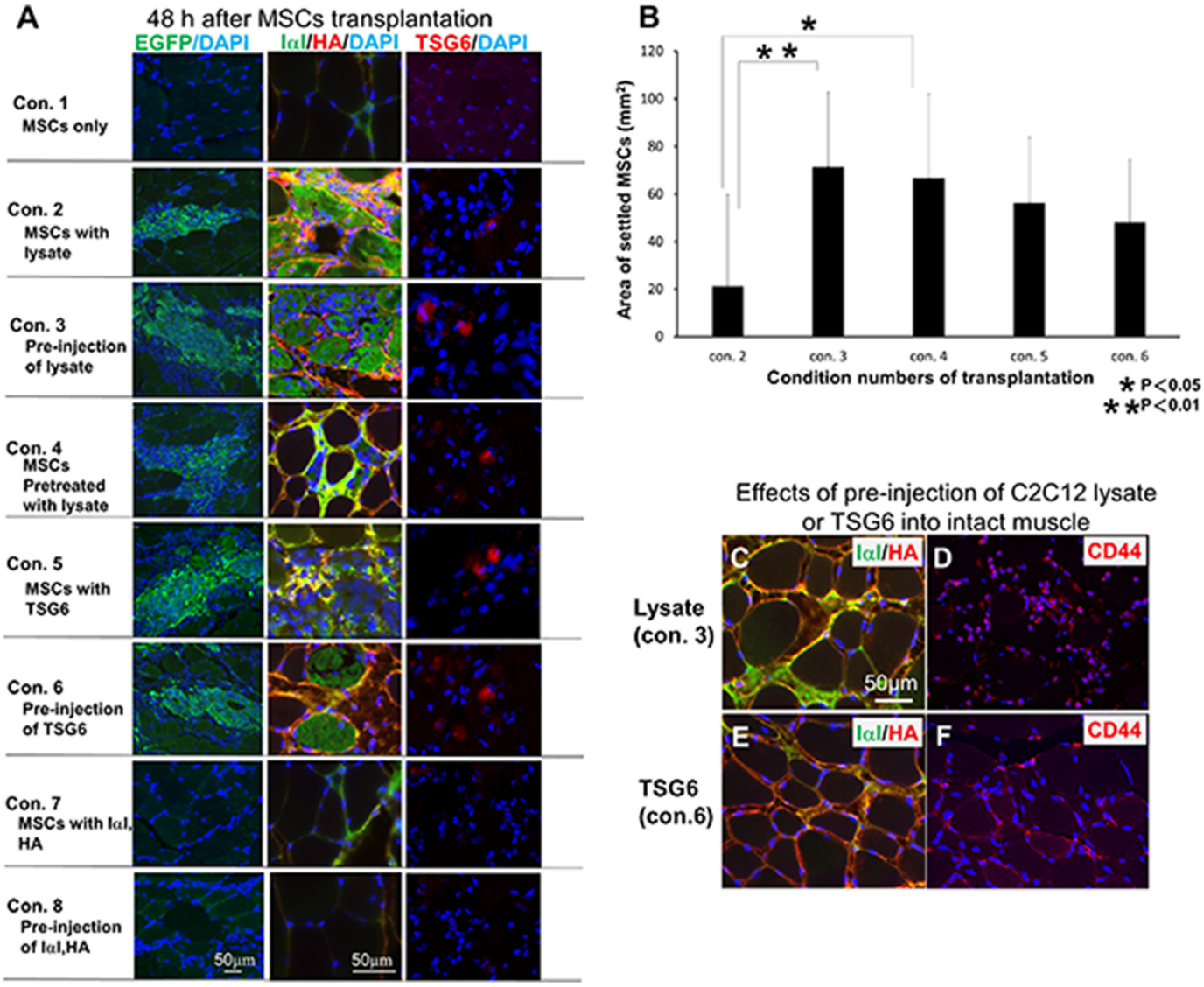

FIGURE 2. **Morphological analysis 48 h after transplantation of MCSs into noninjured skeletal muscle under various conditions.** Eight different conditions for the transplantation are shown in Table 1. *A*, expression of EGFP in *green* (*left column*) indicates the MSCs transplanted. *Middle column* shows expression of IαI (*green*) and HA (*red*) in each condition (*Con.*). *Right column* shows TSG6 (*red*) immunoreactivity in each condition. *B*, area where MSCs settled in each condition were calculated and compared with each other. Under conditions 3 and 6 (see *A* and Table 1) where MSCs were successfully transplanted into the intact muscle tissues, pre-injection of C2C12 lysate (*C* and *D*) and TSG6 (*E* and *F*) increased the expression of IαI (*green*) and HA (*red*) (*C* and *E*) and CD44 (*red*) (*D* and *F*) after 6 h. MSCs transplanted were found to settle in those areas where IαI and HA surrounded muscle fibers and co-localized with each other. *Scale bar* in *A, left bottom panel,* corresponds to all panels in *left column*. *Scale bar* in *A, middle bottom panel,* corresponds to all panels in *middle* and *right columns*. *Scale bar* in *C* corresponds to *C–F* ($n = 3$).

noninjured intact muscle (Fig. 2*A, Con. 4*; Table 1). This finding suggested that lysates of C2C12 stimulated MSCs to express factor(s), which at least partially contributed to the successful settlement of MSCs into noninjured TA muscles.

Lysate of C2C12 Stimulates Expression and Release of TSG6 in MSCs—The above observations revealed the formation of the HA-rich matrices containing the SHAP-HA complex in the injured muscle tissues. The complex has been shown in several reports (18–20, 24, 25, 33, 34) to be formed by the catalytic action of TSG6. During our search for molecules up-regulated by the lysate of C2C12, we therefore speculated that TSG6 could be such a candidate. MSCs were usually maintained in ES-DMEM for a few days before transplantation. At this stage, MSCs expressed TSG6, but the expression was at a low level and the immunoreactivity was restricted around the peri-nuclear regions, as shown in Fig. 3*A*. When lysates of C2C12 were added to ES-DMEM, not only the immunoreactivity of TSG6 became stronger but the distribution pattern also changed significantly from peri-nuclear regions to spreading throughout the cytoplasm (Fig. 3*B*). The expression of TSG6 mRNA in MSCs after addition of the lysate of C2C12 was analyzed by real time PCR and compared with the nontreated MSCs (Fig. 3*C*). Although the amount of TSG6 mRNA in MSCs cultured in ES-DMEM was constant and stable, the amount of TSG6 mRNA altered promptly when MSCs were exposed to lysate of C2C12. It began to increase 3 h after the addition of C2C12 lysate, peaked at 6 h with an 8.4-fold increment, and decreased afterward. It was still 1.4-fold higher at 9 h but was down to a level lower than those in unstimulated MSCs at 12 h. The low level of TSG6 mRNA at least lasted until 48 h after exposure of lysate (Fig. 3*C*).

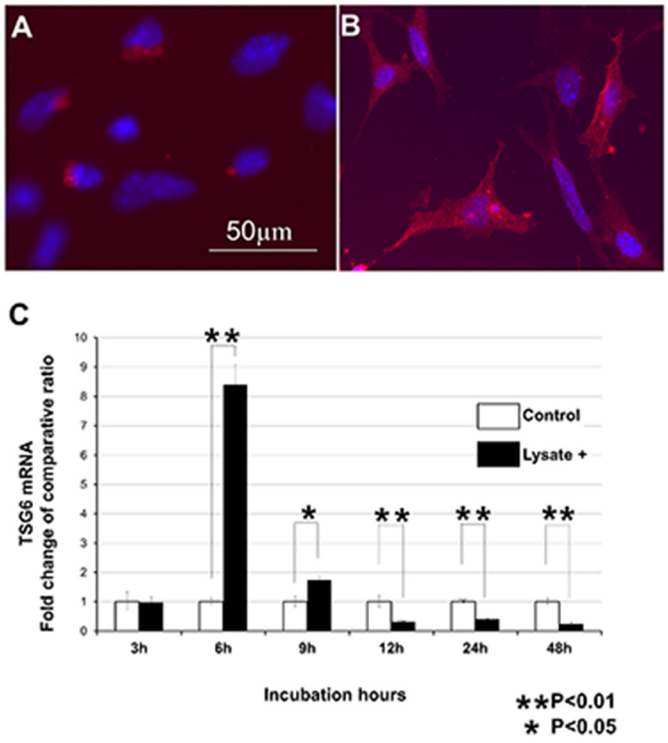

FIGURE 3. **Expression of TSG6 in MSCs after treatment with C2C12 lysate.** MSCs in usual state (*A*) express a small amount of TSG6 immunoreactivity (*red*). The reactivity is located around the nuclei (*blue*). When stimulated by C2C12 lysate, TSG6 immunoreactivity in MSCs increased and expanded throughout their cytoplasm with incubation time (at 48 h, *B*). Expression of TSG6 mRNA was analyzed by real time PCR (*C*). Expression of TSG6 mRNA increased promptly after the addition of C2C12 lysate, peaked at 6 h, and then quickly decreased. *Scale bar* in *A* is the same as in *B* ($n = 4$).

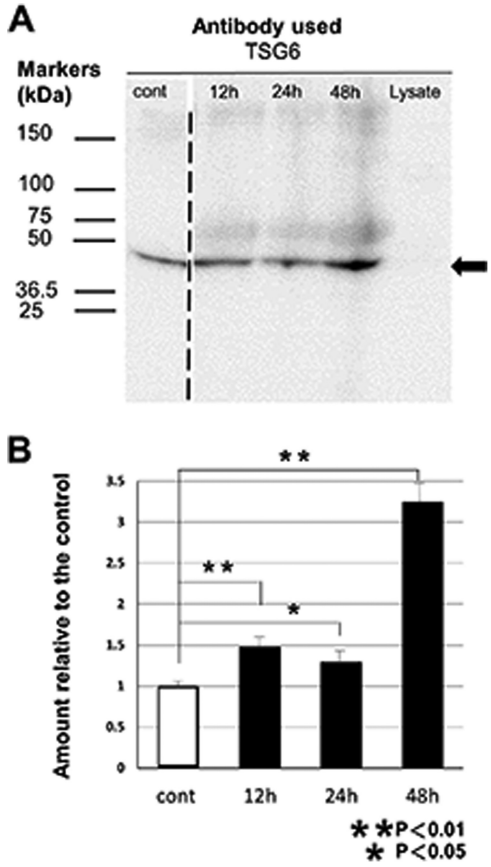

FIGURE 4. **Protein TSG6 released into medium from MSCs by stimulation with C2C12 lysates.** Conditioned medium samples for 12, 24, and 48 h were obtained from MSC cultures incubated for 12, 24, and 48 h, respectively, in medium containing 0.5 mg/ml (protein concentration) lysate of C2C12. The medium sample for the control (*Cont*) was obtained from the culture incubated in normal medium for 48 h. Western blotting analysis for equal amounts of proteins (20 μg) obtained from these conditioned media revealed the presence of TSG6 protein in MSC-conditioned medium (*A*). Lysate of C2C12 did not contain detectable TSG6, but after the addition of C2C12 lysate, protein TSG6 in medium of MSC culture increased. *Arrow* indicates the migrating position of recombinant TSG-6 from R&D Systems. Faint and broad bands with the lower migrating positions than the recombinant TSG-6 may correspond to TSG-6-HCs and TSG-6-IαI and their degraded products (44, 49, 50). The *broken line* between the lanes for the control and for the 12-h cultured medium indicates that there were two lanes in the original figure that contained different amounts (2- and 3-fold) of proteins derived from the control medium cultured for 48 h, and now they were deleted to avoid redundancy. Densities of the probed bands were analyzed using ImagePro software, and integrated densities were normalized to the control medium (mean ± S.D., $n = 3$) (*B*).

We further measured the amount of TSG6 protein in the culture medium by Western blotting (Fig. 4). TSG6 protein was detected in MSC-conditioned medium, but the lysate of C2C12 did not contain any detectable TSG6 protein. When MSCs were stimulated by the lysate of C2C12, MSCs secreted more TSG6 proteins. An apparent increase in the amount of TSG6 protein was observed 12 h after the addition of C2C12 lysate. Collectively, the above data clearly showed that the TSG6 in MSCs is up-regulated by lysate of C2C12.

TSG6 Induces Settlement of MSCs into Noninjured TA Muscle—We therefore explored whether TSG6 plays a role in the settlement of MSCs. The noninjured TA muscle was treated with recombinant TSG6 either simultaneously or 6 h before transplantation of MSCs. Under both conditions, TSG6 successfully induced the settlement of MSCs with an efficiency similar to those of C2C12 lysate administered 6 h before MSC transplantation (Fig. 2, *A, Con. 5* and *6,* and *B*). Pretreatment with recombinant TSG6 or C2C12 lysate increased the expression of IαI, HA, and CD44 at the time point of MSCs transplantation (Fig. 2, *C* and *F*). The results indicated that TSG6 was able to replace the lysate of C2C12 to induce the settlement of MSCs.

We further investigated the involvement of TSG6. We knocked down the expression of TSG6 mRNA in MSCs by introducing TSG6-specific shRNA. The presence of TSG6 shRNA decreased the amount of TSG6 mRNA in MSCs to 30%, even if they were exposed to lysate of C2C12 for 6 h, and the low expression of TSG6 continued for at least 3 days. Immunofluorescent study of TSG6 in MSCs showed extremely reduced expression of TSG6 protein under shRNA (Fig. 5, *C* and *D*). These MSCs were unable to settle in noninjured intact TA muscle after transplantation (Fig. 5). In contrast, control MSCs transfected with noneffective plasmid vector (scrambled plasmid control) settled in the transplanted area. These results suggested that lysate of C2C12 induced MSC settlement into noninjured muscle through up-regulating the expression of TSG6 in MSCs.

Formation of Serum-derived Hyaluronan-associated Protein (SHAP)-HA Complex in the Transplantation Area—We examined here whether the HA-rich matrices mainly consisting of the SHAP-HA complex, which have been shown above to be a major molecular entity, constitute microenvironments specific

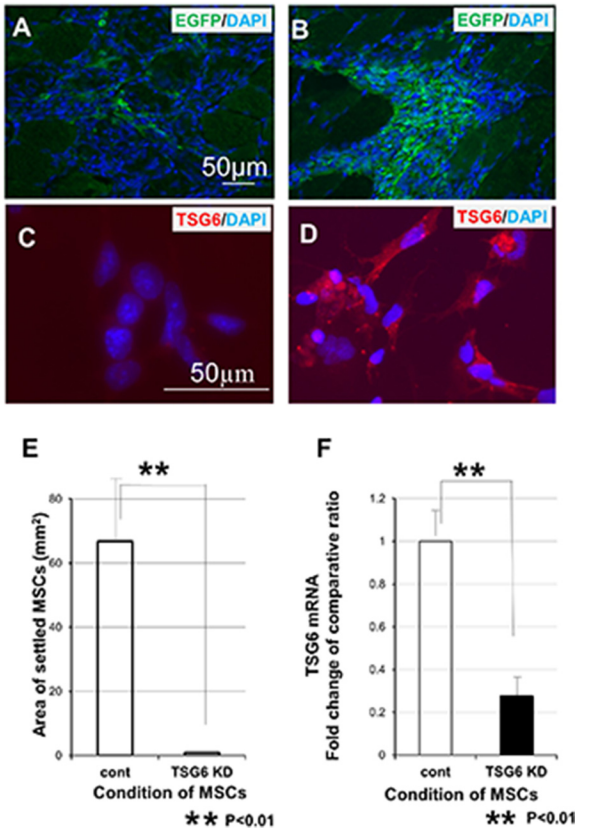

FIGURE 5. **Inhibition of MSC settlement by knockdown of TSG6 (shTSG6).** MSCs knocked down by introducing TSG6-specific shRNA could not be settled in the intact TA muscle after transplantation, even if they were treated and stimulated by lysates of C2C12 for 6 h before transplantation (*A*). However, MSCs transfected with noneffective plasmid vector (scrambled plasmid control) settled in the transplanted area (*B*). Expression of protein TSG6 in MSCs was examined after 6 h of stimulation by C2C12 lysate using immunofluorescent staining. MSCs transfected with TSG6-specific shRNA showed undetectable amount of TSG6 (*C*). MSCs transfected with scrambled plasmid demonstrated high expression of TSG6 (*D*). MSC-settled areas are calculated and compared (*E*). After introducing shRNA into MSCs, the expression of TSG6 mRNA was extremely inhibited, compared with that of the control (*F*). *Scale bar* in *A* is common to *B*. *Scale bar* in *C* is common to *D* ($n = 3$).

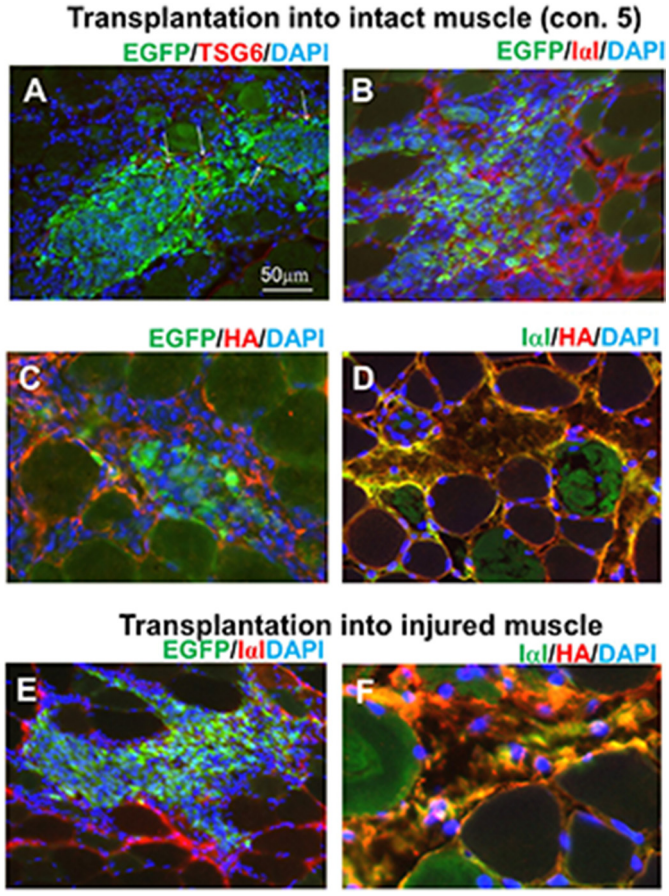

FIGURE 6. **Presence of the SHAP-HA complex surrounding MSCs after transplantation into intact and damaged TA muscle tissues.** After 48 h of successful transplantation of MSCs with TSG6 into the intact muscle (condition 5 in Table 1), a few MSCs of EGFP$^+$ MSCs (*green*) expressed TSG6 (*red*), which were shown to turn *yellow* (see *arrows*) (*A*). In contrast, IαI immunoreactivity (*red*) was expressed at the transplanted area (*green*) (*B*). HA (*red*) also surrounded MSCs (*green*) (*C*). IαI (*green*) and HA (*red*) were co-localized well (see *yellow*) (*D*). When MSCs were transplanted without any addition into the injured muscle tissue, IαI (*red*) was widely observed at the transplanted area (*green*) (*E*). HA (*red*) and IαI (*green*) located closely and demonstrated co-localization (*yellow*) (*F*). *Yellow* surrounding MSCs after transplantation into both intact and damaged TA muscle tissues strongly suggests the presence of the SHAP-HA complex in the area where MSCs were successfully transplanted. *Scale bar* in *A* is common in all panels.

to the damaged skeletal muscle. The SHAP-HA could be preferential substrates for MSCs to settle and regenerate muscle tissues. It has been shown that TSG6 catalyzes the formation of the SHAP-hyaluronan covalent complex from IαI heavy chains and hyaluronan (24, 25), and the complex at the tissue inflammation sites is involved in cell attachment and activation of CD44-bearing lymphocytes and/or resident macrophages (28–30). We checked the presence of the SHAP-HA complex in the transplantation areas. Among the various conditions where the transplantation into noninjured muscles was successfully performed (see Fig. 2 and Table 1), the results obtained in condition 5 were shown here as a typical example (Fig. 6, *A*–*D*). The expression of TSG6 and its surrounding ECM (HA and IαI) was examined by immunostaining in the areas where MSCs were settled 48 h after the transplantation. TSG6 protein in the transplanted MSCs decreased rapidly, and almost disappeared 12 h after transplantation (data not shown). Forty eight h after transplantation, only a trace amount of TSG6 was detected in the transplanted MSCs (Fig. 6*A*). Although the noninjured TA muscle contains no IαI (Fig. 1*A*), the amount of IαI increased greatly after MSC transplantation (Fig. 6*B*). HA was usually distributed in noninjured TA muscle, but the amount was small (Fig. 1*A*). After transplantation of MSCs, HA greatly increased and spread around the MSCs (Fig. 6*C*). Double staining of IαI and hyaluronan showed that the two molecules co-localized well (Fig. 6*D*), suggesting that the SHAP-hyaluronan complex was formed in the transplantation area and may play a key role in the settlement of MSCs. We also examined whether or not MSCs could settle preferentially in the areas where the SHAP-HA complex was localized in the damaged TA muscle. Transplanted GFP$^+$ cells were found in the areas where HA and IαI were co-localized (Fig. 6, *E* and *F*).

Taken together, the transplantation experiments suggested that formation of the SHAP-HA complex was required for the settlement of MSCs after transplantation. Addition of considerable amounts of HA and IαI could not help to settle MSCs, even if they were injected into noninjured intact TA muscle 6 h before MSC transplantation (Fig. 2*A*, *Con. 7* and *8*; Table 1).

Under those conditions, the SHAP-HA complex was not formed because of the lack of TSG6. It indicates that the formation of the SHAP-HA complex in the presence of TSG6 might be important to settle MSCs.

Discussion

We have currently indicated that MSCs from mouse ES cells were settled and differentiated into skeletal muscle cells after their transplantation into injured skeletal muscle (7). However, MSCs could not remain in the transplanted muscle if the muscle had never been damaged, injured, or inflamed, as mentioned regarding the control of this study (Fig. 2*A, Con. 1*; Table 1). The environment of the host tissue is essential for successful transplantation (10, 11, 26).

This study demonstrated clearly that successful transplantations of MSCs into intact TA muscles required lysate of C2C12 (conditions 2 and 3 in Table 1) and pretreatment of MSCs with lysate (condition 4 in Table 1) or TSG6 (conditions 5 and 6 in Table 1). Lysate of C2C12 activated MSCs to express and release TSG6 as shown in Figs. 3 and 4. Therefore, our transplantation conditions 2–6 in Table 1 indicated that the same mechanism involving TSG6 worked to settle MSCs in the intact muscle tissue. In summary, our data suggest that lysate of C2C12 activated MSCs to express and secrete TSG6. We confirmed it by knockdown of TSG6 in MSCs by transfection of shRNA (TSG6). The expression of TSG6 mRNA in MSCs transfected with shRNA decreased, and those unactivated MSCs almost disappeared from the transplanted area. Therefore, TSG6 in MSCs is crucial for settlement after transplantation. In general, cellular injury releases endogenous damage-associated molecular patterns (DAMPs) that activate innate immunity and/or inflammation reactions. DAMPs include surface-exposed calreticulin, secreted ATP, and a released high mobility group of protein B1 and other molecules. Many DAMPs stimulate toll-like receptors (TLR) to initiate inflammation (31, 32). Although we did not identify factors and/or molecules that initiated the expression of TSG6 in our MSCs, DAMPs from C2C12 might be a candidate to induce it through TLR expressed in MSCs. Further investigation is necessary.

Recent reports have indicated that TSG6 transfers heavy chains of IαI to HA and forms the SHAP-HA complex (24, 25, 33, 34). When MSCs released TSG6 in our experiment, both HA and IαI were closely located to the transplanted area, *i.e.* EGFP-positive area. Immunofluorescent double staining of HA and IαI demonstrated that HA and IαI immunoreactivities widely overlapped each other, indicating the formation of the SHAP-HA complex, as described previously (30, 35, 36). TSG6 also increased deposition of HA, and the positive correlation of TSG6 to HA accelerates formation of the SHAP-HA complex (37). When MSCs remained in the intact muscle after transplantation, the complex always surrounded MSCs as shown in Fig. 6. Although the precise formation mechanism of the SHAP-HA complex has not been fully clarified yet, the SHAP-HA complex shows higher cell adhesion activity than HA itself (28, 29, 30). TSG6 generated by activated MSCs formed adhesion molecules of the SHAP-HA complex, and then MSCs were able to settle in the intact TA muscle. We have not performed the direct administration of the SHAP-HA complex with MSCs to settle MSCs in the intact or noninjured muscle. It has been shown that the SHAP-HA complex interacts directly and/or indirectly with various extracellular molecules through protein-protein and/or protein-carbohydrate bindings mediated by other extracellular molecules such as versican/PG-M (38), thrombospondin-1 (39), pentraxin (40–42), and heparan sulfate proteoglycans (43). Such a large extracellular complex (44) might be a real functional entity of the SHAP-HA complex and would be formed only by the encounter of IαI, HA, and TSG-6 in the presence of pericellular and extracellular molecules of MCSs and myotubes. We are now examining those possibilities as our next project.

In our results, it is interesting that the expression of TSG6 mRNA by real time PCR showed a critical time period (6 h) after activation by lysate of C2C12 (Fig. 3*C*). MSCs decreased TSG6 immunoreactivity 12 h after transplantation. The excess amount of the SHAP-HA complex prolongs inflammation by inflammatory cytokines released from wandering cells such as lymphocytes that were accumulated by the SHAP-HA complex (37). An excessive expression of TSG6 interferes with cell differentiation as well (45). Therefore, a short term expression of TSG6 by MSCs enhances their settlement and helps them differentiate into muscle cells. Probably, there is a critical time window for the occurrence of the SHAP-HA complex and the expression of TSG6. This possibility is also suggested by the short term localization of the SHAP-HA complex in the damaged area of the TA muscle after the surgery (see Fig. 1*F* for 48 h and *I* for 1 week).

It is also interesting to know that Coulson-Thomas *et al.* (46) have recently demonstrated that MSCs from umbilical cord express a rich glycocalyx composed of the chondroitin sulfate proteoglycan versican bound to the SHAP-HA complex and could modulate inflammatory cells to reduce the immune response and suppress rejection. This mechanism might be operative in part for the settlement of MSCs transplanted in the damaged muscle and for that of MSCs injected in the intact muscle after activation by the C2C12 lysate, which we observed in this study.

In addition, the SHAP-HA complex may promote myogenic differentiation of MSCs. We previously demonstrated that the SHAP-HA complex is one of the ligands for CD44 (29), and MSCs expressed it after 48 h of transplantation into the injured muscle (data not shown). CD44 activated by ligand binding is internalized and elicits STAT3 (signal transducer and activator of transcription 3) acetylation (47). Price *et al.* (48) currently reported that JAK-STAT3 signaling triggered the myogenic differentiation through cyclin D1 promoter. Despite short time expression of TSG6 in MSCs, the SHAP-HA complex remained longer in the transplanted area suggesting that the SHAP-HA complex may play a role in myogenic differentiation of MSCs (see fetal actin-stained muscle fibers in Fig. 1, *J* and *K*) as well as footholds.

Considering those together, our results demonstrate that TSG6 itself or its release from activated MSCs is important to form the SHAP-HA complex with HA and IαI, which plays a key role in foothold formation of MSCs transplanted not only into injured skeletal muscle but also into intact skeletal muscle.

Author Contributions—S. T. conceived and coordinated the whole study and wrote and edited the paper. M. H., Y. K., K. K. O., M. N., Y. H., Y. K., N. T.-N., and O. W., as students or graduate students, designed, performed, and analyzed the experiments in all figures. L. Z. provided technical information and contributed to coordinating the experiments in Figs. 3–5. K. K. I. directed parts of the study and wrote and edited the paper. All authors reviewed the results and approved the final version of the manuscript.

Acknowledgments—We thank Dr. Niwa (Riken, Kobe, Japan) for the generous gift of mouse ES cells. We also thank Drs. Nakamura and Shinjyo (Seikagaku Co.) for their generous support, Dr. Prachya Kongtawelert (Chiang Mai University, Thailand) for the useful discussion, and Prof. Ushida (Multidisciplinary Pain Center, Aichi Medical University, Japan) for continuous and generous support.

References

1. Awaya, T., Kato, T., Mizuno, Y., Chang, H., Niwa, A., Umeda, K., Nakahata, T., and Heike, T. (2012) Selective development of myogenic mesenchymal cells from human embryonic and induced pluripotent stem cells. *PLoS ONE* **7,** e51638
2. de la Garza-Rodea, A. S., van der Velde-van Dijke, I., Boersma, H., Gonçalves, M. A., van Bekkum, D. W., de Vries, A. A., and Knaän-Shanzer, S. (2012) Myogenic properties of human mesenchymal stem cells derived from three different sources. *Cell Transplant.* **21,** 153–173
3. Goudenege, S., Lebel, C., Huot, N. B., Dufour, C., Fujii, I., Gekas, J., Rousseau, J., and Tremblay, J. P. (2012) Myoblasts derived from normal hESCs and dystrophic hiPSCs efficiently fuse with existing muscle fibers following transplantation. *Mol. Ther.* **20,** 2153–2167
4. Tran, T., Andersen, R., Sherman, S. P., and Pyle, A. D. (2013) Insights into skeletal muscle development and applications in regenerative medicine. *Int. Rev. Cell Mol. Biol.* **300,** 51–83
5. Hwang, Y., Suk, S., Lin, S., Tierney, M., Du, B., Seo, T., Mitchell, A., Sacco, A., and Varghese, S. (2013) Directed *in vitro* myogenesis of human embryonic stem cells and their *in vivo* engraftment. *PLoS ONE* **8,** e72023
6. Ninagawa, N., Murakami, R., Isobe, E., Tanaka, Y., Nakagawa, H., and Torihashi, S. (2011) Mesenchymal stem cells originating from ES cells show high telomerase activity and therapeutic benefits. *Differentiation* **82,** 153–164
7. Ninagawa, N. T., Isobe, E., Hirayama, Y., Murakami, R., Komatsu, K., Nagai, M., Kobayashi, M., Kawabata, Y., and Torihashi, S. (2013) Transplantated mesenchymal stem cells derived from embryonic stem cells promote muscle regeneration and accelerate functional recovery of injured skeletal muscle. *Biores. Open Access* **2,** 295–306
8. Santa María, L., Rojas, C. V., and Minguell, J. J. (2004) Signals from damaged but not undamaged skeletal muscle induce myogenic differentiation of rat bone marrow-derived mesenchymal stem cells. *Exp. Cell Res.* **300,** 418–426
9. Kuraitis, D., Giordano, C., Ruel, M., Musarò, A., and Suuronen, E. J. (2012) Exploiting extracellular matrix-stem cell interactions: a review of natural materials for therapeutic muscle regeneration. *Biomaterials* **33,** 428–443
10. Calve, S., Odelberg, S. J., and Simon, H. G. (2010) A transitional extracellular matrix instructs cell behavior during muscle regeneration. *Dev. Biol.* **344,** 259–271
11. Calve, S., and Simon, H. G. (2012) Biochemical and mechanical environment cooperatively regulates skeletal muscle regeneration. *FASEB J.* **26,** 2538–2545
12. Tran, T. H., Shi, X., Zaia, J., and Ai, X. (2012) Heparan sulfate 6-*O*-endosulfatases (Sulfs) coordinate the Wnt signaling pathways to regulate myoblast fusion during skeletal muscle regeneration. *J. Biol. Chem.* **287,** 32651–32664
13. Mikami, T., Koyama, S., Yabuta, Y., and Kitagawa, H. (2012) Chondroitin sulfate is a crucial determinant for skeletal muscle development/regeneration and improvement of muscular dystrophies. *J. Biol. Chem.* **287,** 38531–38542
14. Casar, J. C., Cabello-Verrugio, C., Olguin, H., Aldunate, R., Inestrosa, N. C., and Brandan, E. (2004) Heparan sulfate proteoglycans are increased during skeletal muscle regeneration: requirement of syndecan-3 for successful fiber formation. *J. Cell Sci.* **117,** 73–84
15. Hunt, L. C., Gorman, C., Kintakas, C., McCulloch, D. R., Mackie, E. J., and White, J. D. (2013) Hyaluronan synthesis and myogenesis: a requirement for hyaluronan synthesis during myogenic differentiation independent of pericellular matrix formation. *J. Biol. Chem.* **288,** 13006–13021
16. Milner, C. M., and Day, A. J. (2003) TSG-6: a multifunctional protein associated with inflammation. *J. Cell Sci.* **116,** 1863–1873
17. Milner, C. M., Higman, V. A., and Day, A. J. (2006) TSG-6: a pluripotent inflammatory mediator? *Biochem. Soc. Trans.* **34,** 446–450
18. Baranova, N. S., Nilebäck, E., Haller, F. M., Briggs, D. C., Svedhem, S., Day, A. J., and Richter, R. P. (2011) The inflammation-associated protein TSG-6 cross-links hyaluronan via hyaluronan-induced TSG-6 oligomers. *J. Biol. Chem.* **286,** 25675–25686
19. Trzeciak, P., Rapała, Ł., Starzyński, R., Dąbrowski, S., and Duszewska, A. M. (2012) TSG-6 protein and its role during maturation of ovarian follicles. *Postepy Hig. Med. Dosw.* **6,** 543–548
20. Swaidani, S., Cheng, G., Lauer, M. E., Sharma, M., Mikecz, K., Hascall, V. C., and Aronica, M. A. (2013) TSG-6 protein is crucial for the development of pulmonary hyaluronan deposition, eosinophilia, and airway hyperresponsiveness in a murine model of asthma. *J. Biol. Chem.* **288,** 412–422
21. Heng, B. C., Gribbon, P. M., Day, A. J., and Hardingham, T. E. (2008) Hyaluronan binding to link module of TSG-6 and to G1 domain of aggrecan is differently regulated by pH. *J. Biol. Chem.* **283,** 32294–32301
22. Kuznetsova, S. A., Mahoney, D. J., Martin-Manso, G., Ali, T., Nentwich, H. A., Sipes, J. M., Zeng, B., Vogel, T., Day, A. J., and Roberts, D. D. (2008) TSG-6 binds via its CUB_C domain to the cell-binding domain of fibronectin and increases fibronectin matrix assembly. *Matrix Biol.* **27,** 201–210
23. Yingsung, W., Zhuo, L., Morgelin, M., Yoneda, M., Kida, D., Watanabe, H., Ishiguro, N., Iwata, H., and Kimata, K. (2003) Molecular heterogeneity of the SHAP-hyaluronan complex. Isolation and characterization of the complex in synovial fluid from patients with rheumatoid arthritis. *J. Biol. Chem.* **278,** 32710–32718
24. Tan, K. T., Baildam, A. D., Juma, A., Milner, C. M., Day, A. J., and Bayat, A. (2011) Hyaluronan, TSG-6, and inter-α-inhibitor in periprosthetic breast capsules: reduced levels of free hyaluronan and TSG-6 expression in contracted capsules. *Aesthet. Surg. J.* **31,** 47–55
25. Zhang, S., He, H., Day, A. J., and Tseng, S. C. (2012) Constitutive expression of inter-α-inhibitor (IαI) family proteins and tumor necrosis factor-stimulated gene-6 (TSG-6) by human amniotic membrane epithelial and stromal cells supporting formation of the heavy chain-hyaluronan (HC-HA) complex. *J. Biol. Chem.* **287,** 12433–12444
26. Kvezereli, M., Michie, S. A., Yu, T., Creusot, R. J., and Fontaine, M. J. (2008) TSG-6 protein expression in the pancreatic islets of NOD mice. *J. Mol. Histol.* **39,** 585–593
27. Di Battista, A. P., and Locke, M. (2013) Isolated hearts treated with skeletal muscle homogenates exhibit altered function. *Cell Stress Chaperones* **18,** 675–681
28. Choi, H., Lee, R. H., Bazhanov, N., Oh, J. Y., and Prockop, D. J. (2011) Anti-inflammatory protein TSG-6 secreted by activated MSCs attenuates zymosan-induced mouse peritonitis by decreasing TLR2/NF-κB signaling in resident macrophages. *Blood* **118,** 330–338
29. Zhuo, L., Kanamori, A., Kannagi, R., Itano, N., Wu, J., Hamaguchi, M., Ishiguro N., and Kimata, K. (2006) SHAP potentiates the CD44-mediated leukocyte adhesion to the hyaluronan substratum. *J. Biol. Chem.* **281,** 20303–20314
30. McDonald, B., Jenne, C. N., Zhuo, L., Kimata, K., and Kubes, P. (2013) Kupffer cells and activation of endothelial TLR4 coordinate neutrophil adhesion within liver sinusoids during endotoxemia. *Am. J. Physiol. Gastrointest. Liver Physiol.* **305,** G797–G806
31. Zhang, Q., Raoof, M., Chen, Y., Sumi, Y., Sursal, T., Junger, W., Brohi, K., Itagaki, K., and Hauser, C. J. (2010) Circulating mitochondrial DAMPs cause inflammatory responses to injury. *Nature* **464,** 104–107
32. Krysko, D. V., Garg, A. D., Kaczmarek, A., Krysko, O., Agostinis, P., and

Vandenabeele, P. (2012) Immunogenic cell death and DAMPs in cancer therapy. *Nat. Rev. Cancer* **12,** 860–875
33. Baranova, N. S., Foulcer, S. J., Briggs, D. C., Tilakaratna, V., Enghild, J. J., Milner, C. M., Day, A. J., and Richter, R. P. (2013) Inter-α-inhibitor impairs TSG-6-induced hyaluronan cross-linking. *J. Biol. Chem.* **288,** 29642–29653
34. Lauer, M. E., Glant, T. T., Mikecz, K., DeAngelis, P. L., Haller, F. M., Husni, M. E., Hascall, V. C., and Calabro, A. (2013) Irreversible heavy chain transfer to hyaluronan oligosaccharides by tumor necrosis factor-stimulated gene-6. *J. Biol. Chem.* **288,** 205–214
35. Zhuo, L., Hascall, V. C., and Kimata, K. (2004) Inter-α-trypsin inhibitor, a covalent protein-glycosaminoglycan-protein complex. *J. Biol. Chem.* **279,** 38079–38082
36. Lesley, J., Gál, I., Mahoney, D. J., Cordell, M. R., Rugg, M. S., Hyman, R., Day, A. J., and Mikecz, K. (2004) TSG-6 modulates the interaction between hyaluronan and cell surface CD44. *J. Biol. Chem.* **279,** 25745–25754
37. Lauer, M. E., Cheng, G., Swaidani, S., Aronica, M. A., Weigel, P. H., and Hascall, V. C. (2013) Tumor necrosis factor-stimulated gene-6 (TSG-6) amplifies hyaluronan synthesis by airway smooth muscle cells. *J. Biol. Chem.* **288,** 423–431
38. Zhuo, L., and Kimata, K. (2008) Structure and function of inter-α-trypsin inhibitor heavy chains. *Connect Tissue Res.* **49,** 311–320
39. Kuznetsova, S. A., Day, A. J., Mahoney, D. J., Rugg, M. S., Mosher, D. F., and Roberts, D. D. (2005) The N-terminal module of thrombospondin-1 interacts with the link domain of TSG-6 and enhances its covalent association with the heavy chains of inter-α-trypsin inhibitor. *J. Biol. Chem.* **280,** 30899–30908
40. Zhang, S., Zhu, Y. T., Chen, S. Y., He, H., and Tseng, S. C. (2014) Constitutive expression of pentraxin 3 (PTX3) protein by human amniotic membrane cells leads to formation of the heavy chain (HC)-hyaluronan (HA)-PTX3 complex. *J. Biol. Chem.* **289,** 13531–13542
41. Ievoli, E., Lindstedt, R., Inforzato, A., Camaioni, A., Palone, F., Day, A. J., Mantovani, A., Salvatori, G., and Salustri, A. (2011) Implication of the oligomeric state of the N-terminal PTX3 domain in cumulus matrix assembly. *Matrix Biol.* **30,** 330–337
42. Maina, V., Cotena, A., Doni, A., Nebuloni, M., Pasqualini, F., Milner, C. M., Day, A. J., Mantovani, A., and Garlanda, C. (2009) Coregulation in human leukocytes of the long pentraxin PTX3 and TSG-6. *J. Leukocyte Biol.* **86,** 123–132
43. Ujita, M., Shinomura, T., Ito, K., Kitagawa, Y., and Kimata, K. (1994) Expression and binding activity of the carboxyl-terminal portion of the core protein of PG-M, a large chondroitin sulfate proteoglycan. *J. Biol. Chem.* **269,** 27603–27609
44. Evanko, S. P., Tammi, M. I., Tammi, R. H., and Wight, T. N. (2007) Hyaluronan-dependent pericellular matrix. *Adv. Drug. Deliv. Rev.* **59,** 1351–1365
45. Tsukahara, S., Ikeda, R., Goto, S., Yoshida, K., Mitsumori, R., Sakamoto, Y., Tajima, A., Yokoyama, T., Toh, S., Furukawa, K., and Inoue, I. (2006) Tumour necrosis factor α-stimulated gene-6 inhibits osteoblastic differentiation of human mesenchymal stem cells induced by osteogenic differentiation medium and BMP-2. *Biochem. J.* **398,** 595–603
46. Coulson-Thomas, V. J., Gesteira, T. F., Hascall, V., and Kao, W. (2014) Umbilical cord mesenchymal stem cells suppress host rejection: the role of the glycocalyx. *J. Biol. Chem.* **289,** 23465–23481
47. Lee, J. L., Wang, M. J., and Chen, J. Y. (2009) Acetylation and activation of STAT3 mediated by nuclear translocation of CD44. *J. Cell Biol.* **185,** 949–957
48. Price, F. D., von Maltzahn, J., Bentzinger, C. F., Dumont, N. A., Yin, H., Chang, N. C., Wilson, D. H., Frenette, J., and Rudnicki, M. A. (2014) Inhibition of JAK-STAT signaling stimulates adult stellite cell function. *Nat. Med.* **20,** 1174–1181
49. He, H., Li, W., Tseng, D. Y., Zhang, S., Chen, S. Y., Day, A. J., and Tseng, S. C. (2009) Biochemical characterization and function of complexes formed by hyaluronan and the heavy chains of inter-α-inhibitor (HC-HA) purified from extracts of human amniotic membrane. *J. Biol. Chem.* **284,** 20136–20146
50. Rugg, M. S., Willis, A. C., Mukhopadhyay, D., Hascall, V. C., Fries, E., Fülöp, C., Milner, C. M., and Day, A. J. (2005) Characterization of complexes formed between TSG-6 and inter-α-inhibitor that act as intermediates in the covalent transfer of heavy chains onto hyaluronan. *J. Biol. Chem.* **280,** 25674–25686